ANALYSIS OF GNSS-R COVERAGE BY A REGIONAL AIRCRAFT FLEET

Ryan Linnabary[1], Andrew O'Brien[1], Chris Ruf[2], Stephen Musko[2], Delwyn Moller[3]

[1]The Ohio State University, Columbus, OH, USA
[2]University of Michigan, Ann Arbor, MI, USA
[3]University of Auckland, Auckland, New Zealand

ABSTRACT

Airborne GNSS-R instrument systems are typically only utilized for a limited number of aircraft flights to perform experiments, to test new instruments, or to collect data over specific targets (i.e. hurricanes). A new system is currently under consideration whereby GNSS-R instruments could be permanently installed on a fleet of regional aircraft. This is a novel and ambitious concept that offers fascinating and powerful system for collecting science information over a large spatial region and short temporal scales. Here we present an exploratory analysis meant to quantify the merit of such a system as applied to the Air New Zealand Q300 regional aircraft. Simulations using realistic flight paths combined with GNSS orbit information are used to simulate GNSS-R measurement coverage. Results confirm the exciting potential of a next-generation GNSS-R receiver in this scenario.

***Index Terms*—** GNSS Reflectometry, Bistatic radar

1. BACKGROUND

Global Navigational Satellite System Reflectometry (GNSS-R) utilizes GNSS signals reflected off of the Earth to provide a large variety of scientific information. NASA's Cyclone Global Navigational Satellite System (CYGNSS) Mission, composed of 8 micro-satellites, is the most well known spaceborne GNSS-R system. Airborne GNSS-R systems are also widely used to perform experiments [1-4], but, unlike spaceborne systems, their usage has always been limited to a small number of flights. Recently, the University of Auckland – in partnership with Air New Zealand (ANZ) and the University of Michigan (UM) – is exploring an exciting new possibility of permanently deploying GNSS-R instruments on a fleet of small regional aircraft. The GNSS-R instrument would be the Next-Generation GNSS-R Receiver (NGRx), which is currently finalizing development by UM as part of a NASA Instrument Incubator Program (IIP). Small, aircraft-certified GNSS antennas would be mounted on the top and bottom of the aircraft to capture direct-path and reflected-path signals, respectively. A preliminary analysis was performed in order to understand the GNSS-R instrument's measurement coverage. A subset of the results from this analysis are shared here.

2. AIRCRAFT FLIGHT PATH ANALYSIS

Figure 1(a) shows a photo of the Air Nelson Bombardier Q300 aircraft that is under consideration. Currently, 23 of these aircraft are in service. Figure 1(b) shows a map of New

(a) Air New Zealand Q300 Aircraft

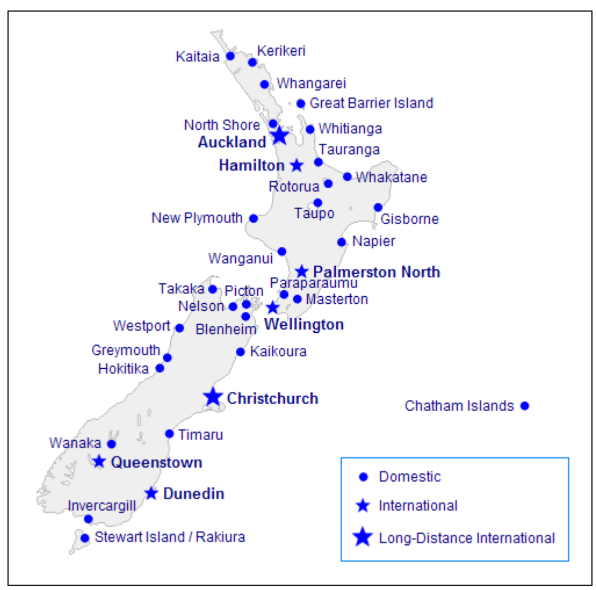

(b) New Zealand Airport Map

Fig. 1: Aircraft under consideration for GNSS-R instrument installation (a) and locations of New Zealand airports (b).

	Auckland	Wellington	Christchurch
Kerikeri	67	0	0
Whangarei	58	0	0
Tauranga	89	55	37
Hamilton	0	14	0
Rotorua	49	45	0
Taupo	33	0	0
Gisborne	73	31	0
Napier	14	55	0
N. Plymouth	59	46	29
Palmerston N.	14	20	0
Nelson	31	134	73
Blenheim	69	66	0
Hokitika	0	0	28
Timaru	0	29	0
Dunedin	0	0	2
Invercargill	0	24	4

Fig. 2: Typical annual routes for a single ANZ Q300 aircraft showing number of flights between New Zealand airports.

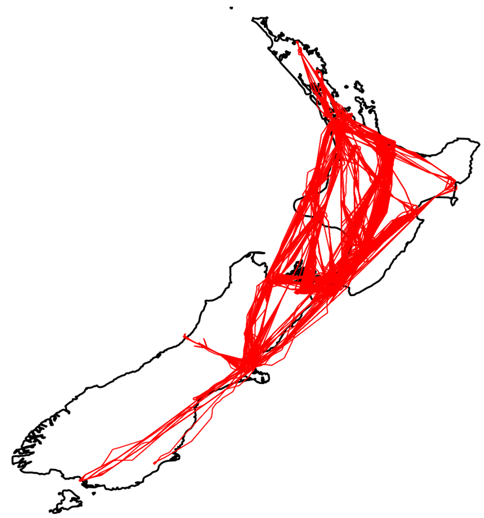

Fig. 3: Flight paths from FlightAware of all ANZ Q-300 aircraft over one week.

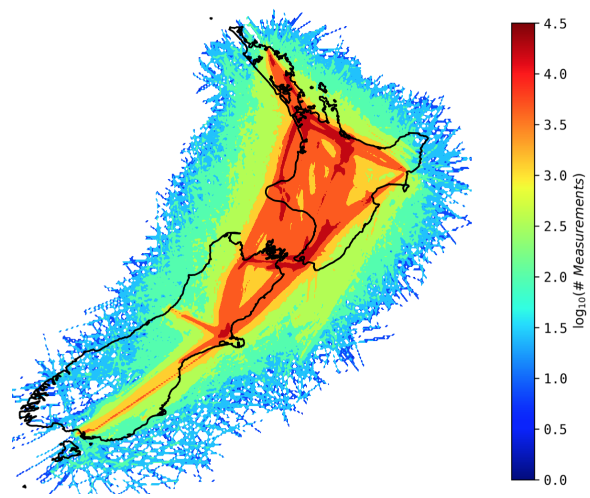

Fig. 4: One week of GNSS-R measurements for the ANZ Q300 aircraft fleet, showing measurement count in log-scale. Results are comparable to a single Q300 aircraft accumulated over a year.

Zealand and the location of various regional and international airports. The Q300 aircraft operate frequent flights between most (though not all) of these airports. Table 2 indicates a the number of flights in a year a typical Q300 makes.

Figure 3 shows the flight paths from of all ANZ Q-300 aircraft over one week. ADS-B data for actual Q300 flights were obtained from FlightAware for October 23-30, 2019 [5]. The total number of flights over this week was 1135 flights. This was a particularly busy week as the annual number of flights for a single Q300 aircraft is estimated to be 1268 flights. Thus, for our analysis, the coverage of this 1 week of all Q300 aircraft will be very similar to 1 year of a single aircraft. Work was done to condition this data for our GNSS-R simulations, as it contained position and ground speed with an irregular frequency. The flight path data was interpolated to one-second resolution, and velocity was calculated as differential position. Aircraft attitude frames were established with some assumptions based on the velocity vector.

GNSS-R measurement coverage was simulated assuming tracking of a single signal type from GPS, Galileo, Beidou, and QZSS constellations [6]. To solve for the specular points, actual flight path data over one week were used to serve as the position and attitude for the receiver, and IGS data provided the transmitter location information. Measurements were assumed to be taken at 1 Hz, although the actual rate of the instrument could be higher.

Figure 4 shows the GNSS-R measurements for the ANZ Q300 aircraft fleet accumulated over 1 week. The measurements are counted in 5 km grid cells. Since the number of measurements is very dense near airports (due to the high traffic and low flight altitudes), the measurement count in the figure is shown in log-scale. Again, it should be noted that these results are comparable to the measurements from a single Q300 aircraft accumulated over a year. We find that, on average, each Q300 flight lasts 45 minutes and accumulates $81,000$ measurements. It should be noted that our simulation does not account for topology, so the measurement density over the western mountainous areas are over-represented in this figure. Nonetheless, the coverage and density of measurements is substantial and compelling.

To better understand the temporal sampling of a typical area, Figure 5 shows the GNSS-R measurements versus time that occur over Lake Taupo near the center of the northern New Zealand. The top stem plot shows the sampling over 1 week, and highlights that there is regular sampling over the

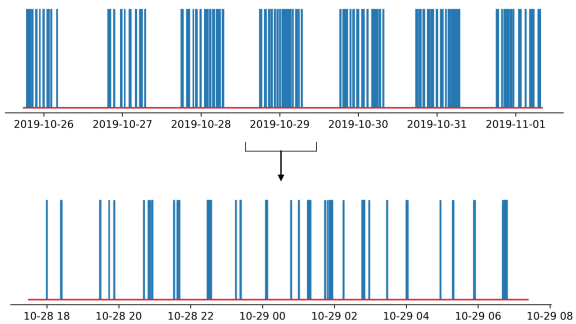

Fig. 5: Temporal sampling of GNSS-R measurements over Lake Taupo versus time (UTC) showing one week (top) and a closer view of a single day (bottom).

course of a day and gaps during the night. The bottom figure shows a zoomed in view of the daytime portion of a single day indicating a sub-hourly revisit rate. This behavior is typical of red and orange portions of the map in Figure 4.

3. ANALYSIS OF A SINGLE FLIGHT

To offer a more clear understanding of the GNSS-R measurements expected from the system, we will look closer at a single flight. Figure 6 shows the flight path (red line) of a single ANZ Q300 flight from Tauranga to Christchurch (southward). Blue lines indicate the locations of GNSS reflection specular points. We observe that most of the measurements are concentrated around the flight path, although there are also occasional tracks available closer to the horizon that are a farther distance away.

Figure 7 shows the altitude and ground speed of the flight. This profile is typical of ANZ Q300 flights, with a cruising altitude of approximately 20,000 ft and a ground speed of 250

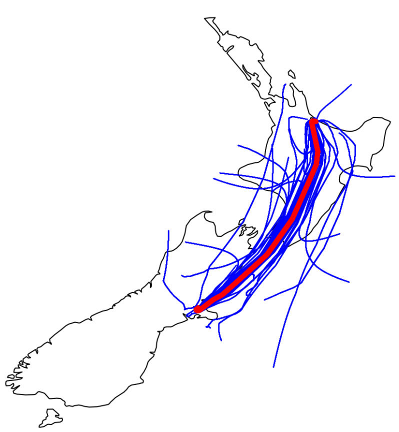

Fig. 6: Example ANZ Q300 flight From Tauranga to Christchurch

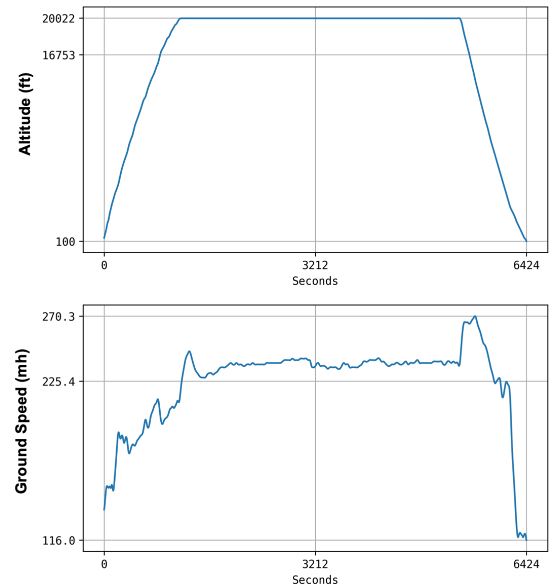

Fig. 7: The altitude and ground speed of the example flight based on ADS-B data.

mph. This flight was 107 minutes in duration with the ascending and descending portions of the flight occupying nearly one third of the flight time.

Figure 8 shows the directions of GNSS satellites over the entire flight in the aircraft body frame. The top plot shows the upper hemisphere and the direction of direct-path signals. The bottom plot shows the lower hemisphere and the directions of reflection-path signals. The azimuth-elevation polar coordinate system indicates the front (F), back (B), left (L) and right (R) of the aircraft. Due to the aircraft's low altitude as compared to a CYGNSS satellite, the directions in the upper and lower hemispheres are nearly mirror images of each other, with the only noticeable differences occurring near the horizon or when the aircraft attitude changes during the ascending or descending phases. Jagged lines in these plots are caused by brief adjustments in yaw throughout the flight. Near airports, when the aircraft altitude is low, measurements will occur very close to the aircraft location. At cruising altitude, the reflections will be visible all the way to the horizon (the horizon is 278km away at a 20,000 ft altitude).

Figure 9 quantifies the number of available GNSS-R measurements versus time for the GPS and Galileo constellations. In this case, they have been divided into three groups based on their incidence angle (indicated by color). We can see that the majority of measurements are less than 60 deg. incidence angle, which is the typical range of measurements from instruments like CYGNSS. However, there is also a significant number at higher incidences between 60 and 80 degrees and exceeding 80 degrees (i.e. grazing incidence). At these angles, we expect different behavior in the GNSS reflection in terms of different polarization and with increasing coherence.

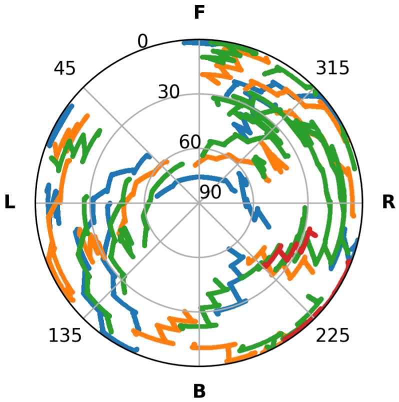

(a) Upper Hemisphere - Direct Path GNSS

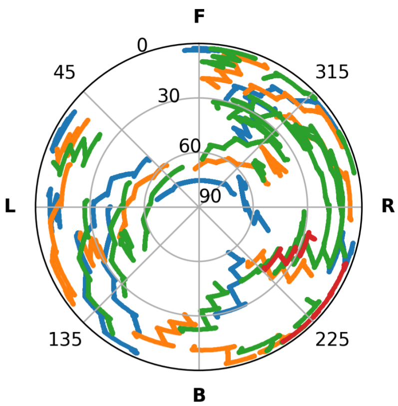

(b) Lower Hemisphere - GNSS Reflections

Fig. 8: Azimuth and elevation directions to GNSS signals in the aircraft coordinate frame during the example flight for the upward-looking antenna (top) and the downward-looking antenna (bottom).

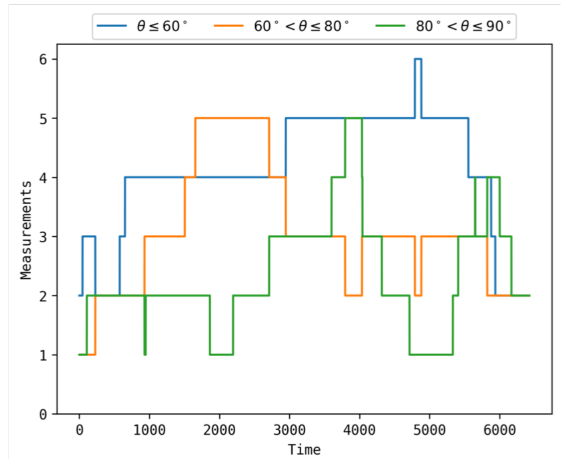

(a) GPS

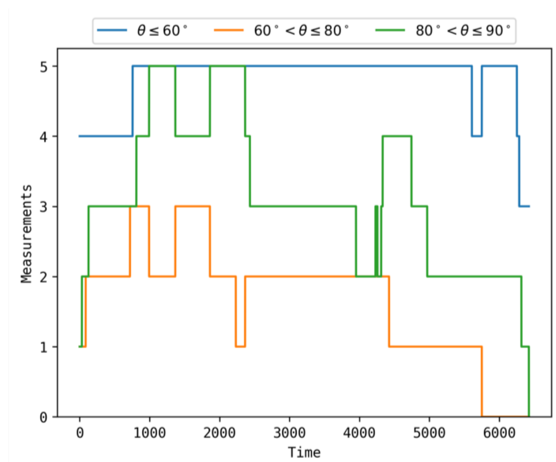

(b) Galileo

Fig. 9: The number of available GNSS-R measurements versus time during the example flight. Results are divided by incidence angle range (θ) separately for the GPS and Galileo constellations.

Additional details of our analysis will be presented, including expected quality of the GNSS-R measurements (i.e. SNR) given the instrument and antenna configuration on the aircraft as well as a summary of the science potential, relating coverage to New Zealand land types [7].

4. REFERENCES

[1] Garrison, James L. et al. "Effect of sea roughness on bistatically scattered range coded signals from the Global Positioning System," IEEE Geophysical Research Letters, vol 25, no. 30, pg 2257-2260, July 1998.

[2] Lowe, Stephen T. et al. "5-cm-Precision aircraft ocean altimetry using GPS reflections," IEEE Geophysical Research Letters vol 29, no. 10. pg. 1375-1385, May 2002.

[3] Ralf Stosius et al., "GNSS-R Mission Planning Aboard the Research Aircraft HALO," *2010 IEEE Specialist Meeting on GNSS Reflectometry*, Barcelona, Spain, October 21-22, 2010.

[4] E. Cardellach et al., "Wetland GNSS-R measurements from aircraft," *2017 IEEE International Geoscience and Remote Sensing Symposium (IGARSS)*, Fort Worth, TX, 2017, pp. 1122-1125.

[5] FlightAware - Global Flight Tracker Product *https://flightaware.com/*.

[6] CYGNSS End-to-End Simulator Technical Memo. Space Physics Research Laboratory, 2015. *http://clasp-research.engin.umich.edu/missions/cygnss/reference/148-0123_CYGNSS_E2ES_EM.pdf*

[7] Landcare Research - New Zealand Land Cover Database Version 4.1. July 2015. *https://lris.scinfo.org.nz*.